Molecular Biology and Evolution

Contrasting Modes of Evolution of the Visual Pigments in *Heliconius* Butterflies

Furong Yuan,[1] Gary D. Bernard,[2] Jennifer Le,[1] and Adriana D. Briscoe*[,1]

[1]Department of Ecology and Evolutionary Biology, University of California, Irvine

[2]Department of Electrical Engineering, University of Washington, Seattle

***Corresponding author:** E-mail: abriscoe@uci.edu.

Associate editor: Patricia Beldade

Data deposition: The sequences reported in this article have been deposited in the GenBank database (accession nos. GU324674–GU324705).

Abstract

The adult compound eyes of passion-vine butterflies in the genus *Heliconius* contain one more UV opsin than other butterflies. Together with an 11-*cis*-3-hydroxyretinal chromophore, their four opsin genes *UVRh1*, *UVRh2*, *BRh*, and *LWRh* produce four rhodopsins that are UV-, blue-, or long wavelength absorbing. One of the *Heliconius* UV opsin genes, *UVRh2*, was found to have evolved under positive selection following recent gene duplication, using the branch-site test of selection. Using a more conservative test, the small-sample method, we confirm our prior finding of positive selection of *UVRh2* and provide new statistical evidence of episodic evolution, that is, positive selection followed by purifying selection. We also newly note that one of the positively selected amino acid sites contains substitutions with known spectral tuning effects in avian ultraviolet- and violet-sensitive visual pigments. As this is one of a handful of described examples of positive selection of any specific gene in any butterfly where functional variation between copies has been characterized, we were interested in examining the molecular and physiological context of this adaptive event by examining the UV opsin genes in contrast to the other visual pigment genes. We cloned *BRh* and *LWRh* from 13 heliconiine species and *UVRh1* and *UVRh2* from *Heliconius elevatus*. In parallel, we performed in vivo epi-microspectrophotometric experiments to estimate the wavelength of peak absorbance, λ_{max}, of several rhodopsins in seven heliconiine species. In contrast to *UVRh2*, we found both physiological and statistical evidence consistent with purifying selection on *UVRh1*, *BRh*, and *LWRh* along the branch leading to the common ancestor of *Heliconius*. These results underscore the utility of combining molecular and physiological experiments in a comparative context for strengthening evidence for adaptive evolution at the molecular level.

Key words: rhodopsin, color vision, adaptive evolution, gene duplication.

Introduction

The rise of the genomic era in biology has led to unprecedented opportunities to study the patterns and processes of molecular evolution. This has led to a proliferation of computational methods, journals, and reports of widespread signatures of positive selection throughout the genomes of prominent model organisms such as *Drosophila melanogaster* (Sella et al. 2009). Nonetheless, a challenge facing all of evolutionary biology includes identifying which of these statistically identified candidates for adaptive evolution represent true examples of positive selection and which represent false positives (Nozawa et al. 2009; Garrigan et al. 2010). An even larger challenge is then to identify the phenotypes of the adaptive variants and their impact on fitness, tasks that are especially difficult for the majority of loci.

Comparative physiology is a relatively old discipline in the life sciences that can provide an experimental paradigm for identifying the phenotypes of newly evolved variants. Conversely, if performed in parallel with genotyping, it can refute claims of adaptive evolution based on statistical evidence alone. Although comparative physiology is necessarily limited to groups of genes that have lent themselves to experimental study (e.g., *melanocortin-1-receptor* [Hoekstra et al. 2006], *cryptochromes* [Yuan et al. 2007], hemoglobins [Storz et al. 2009], *amylase* [Perry et al. 2007]), it is nonetheless worthwhile to explore the extent to which genomics and physiology arrive at similar conclusions, if we are to further our knowledge of the extent of adaptation in nature.

To that end, we have been studying the molecular and phenotypic evolution of the visual pigments, rhodopsins, of butterflies (Briscoe 2008). The visual pigments, or photoreceptor molecules, found in the adult compound eyes are useful for studying the fates of both duplicate genes as well as the fates of new allelic variants at individual loci that arise as the result of adaptation between species. Compared with other insects like bees (Peitsch et al. 1992), a surprising number of opsin gene duplications have arisen that have resulted in novel spectral classes of photoreceptor cell (Arikawa et al. 2005; Frentiu, Bernard, Sison-Mangus, et al. 2007; Wakakuwa et al. 2007). Although the total number of species screened for multiple classes of opsins is still small (40+ species) compared with the estimated number of butterfly species (~15,000), representative species of each of the five butterfly families have been found to have different numbers of opsins due to lineage-specific duplication events of the three basic classes of opsin gene,

ultraviolet (*UVRh*), blue (*BRh*), and long-wavelength (*LWRh*) (Briscoe 2008).

So far, most of the identified duplication events appear to have been ancient and unsuitable for detecting recent episodes of positive selection, even though they were presumably positively selected in the past. For example, the two *BRh* opsin genes of lycaenid butterflies arose before the split between the three most species-rich lycaenid subfamilies but sometime after the split between lycaenid and riodinid families (Sison-Mangus et al. 2006). The three duplicated *LWRh* opsins expressed in the adult compound eye in Papilio butterflies are another example (Briscoe 1998; Kitamoto et al. 1998). The age of these duplication events is such that saturation of synonymous sites has made it difficult to reliably estimate both ancestral sequences and a common metric for identifying positive selection, namely the ratio of nonsynonymous to synonymous substitutions.

In contrast to these old duplications where the processes under which they evolved new functions cannot be reliably reconstructed, we have recently described a new duplication, and evidence of positive selection of an UV opsin gene, *UVRh2*, found only in butterflies of the genus *Heliconius*—one of the few known examples of positive selection for any gene in any butterfly (Briscoe et al. 2010a). Other examples of positively selected genes in butterflies include *phosphoglucose isomerase* (*PGI*) in *Melitaea cinxia*, which appears to have evolved under balancing selection (Wheat et al. 2010), and the long-wavelength (*LWRh*)–absorbing rhodopsin of *Limenitis* butterflies where adaptive variants have become fixed between closely related species (Frentiu, Bernard, Cuevas, et al. 2007). These three genes are of special interest because along with statistical evidence for positive selection, some of the functional variation associated with these loci has been characterized physiologically. Their impact on fitness, at least for the two rhodopsin examples, is not known.

Butterflies of the genus *Heliconius* (Nymphalidae) are considered examples of an adaptive radiation due to the spectacular diversity of mimetic wing color patterns that have evolved in species and races throughout Mexico and Central and South America (Baxter et al. 2010; Counterman et al. 2010). They also have a visual system unlike any other described butterfly. Nymphalid butterflies have eyes that typically contain three spectrally distinct rhodopsins, including one ultraviolet- (λ_{max} = 300–400, UVRh), one blue- (λ_{max} = 400–500, BRh), and one long-wavelength (λ_{max} = 500–600, LWRh)–absorbing rhodopsin encoded by three loci, *UVRh*, *BRh*, and *LWRh* (Briscoe et al. 2003; Sauman et al. 2005). For example, *Dryas iulia*, a close *Heliconius* relative, has eyes that contain three rhodopsins with λ_{max} = 385, 470, and 555 nm, whereas *Heliconius erato* has eyes that contain four rhodopsins with λ_{max} = 355, 398, 470, and 555 nm. *Heliconius erato* eyes also contain four opsin-encoding mRNAs *UVRh1*, *UVRh2*, *BRh*, and *LWRh* in contrast to the usual three found in *D. iulia*. Intriguingly, the gene duplication giving rise to the *UVRh1* and *UVRh2* opsin genes arose at the same time that UV–yellow pigments appeared on the wings of many *Heliconius* butterflies (Briscoe et al. 2010a). Because the closest relatives of *Heliconius* have yellow pigments that lack a UV component and contain eyes with only one UV opsin, this suggests that the duplicate UV opsin genes may have been recruited for species recognition in *Heliconius* (Briscoe et al. 2010).

Because it has been suggested that the statistical test we used to detect positive selection, the branch-site method (Zhang et al. 2005) has a higher-than-expected false-positive rate when the number of substitutions is small (Nozawa et al. 2009, 2010), we were interested in examining an expanded data set using the small-sample method (SSM) and Fisher's exact test (Zhang et al. 1997), which has been shown to be much more conservative in rejecting the null hypothesis of neutral evolution (Nozawa et al. 2009). Also, because a single rhodopsin sometimes functions coordinately with other spectrally distinct classes of rhodopsin in the context of color vision, although not always (see, e.g., Koshitaka et al. 2008), there is the possibility that selection for spectral tuning of one visual pigment may have resulted in selection for spectral tuning of other visual pigments. We were therefore interested in investigating the possibility that selection on the *Heliconius* clade-specific *UVRh2* gene may have resulted in compensatory evolution in the genes encoding other spectral classes of opsins. Lastly, we performed new physiological experiments that together with prior studies have allowed us to examine the extent to which a statistical and physiological approach reach the same conclusions about the evolution of heliconiine opsins.

Materials and Methods

Taxonomic Sampling

Heliconiine specimens targeted for screening of rhodopsin mRNAs were either collected in localities in the United States, Mexico, Costa Rica, and Peru or provided to us from laboratory colonies established from source material in Costa Rica (supplementary table S1, Supplementary Material online). Adult butterflies were preserved by either storing in RNALater or snap freezing in liquid nitrogen. The *Speyeria leto* butterfly used for the epi-microspectrophotometry experiment described below was preserved as a dried specimen. Because butterfly *UVRh* and *BRh* opsin genes typically have at least eight small exons with very long introns, we did not attempt to clone these undescribed sequences from the dried specimen. We instead compared in our analysis below the opsin sequences previously obtained from cDNA prepared from the related species, *Speyeria mormonia* (Pohl et al. 2009).

Polymerase Chain Reaction and Sequencing of *UVRh*, *BRh*, and *LWRh* Opsin Genes

Total RNAs were extracted from whole heads using Trizol (Invitrogen). One-step reverse transcriptase–polymerase chain reaction (PCR) using AffinityScript multiple temperature cDNA synthesis kit (Stratagene, La Jolla, CA) and proof-reading BD *Taq* polymerase (BD Biosciences, San Jose, CA) was performed on each template to amplify all

four opsin genes from *Heliconius elevatus*, and *BRh* and *LWRh* opsin transcripts from eight additional species in the *Heliconius* genus and three basal heliconids (*Dione moneta*, *D. iulia*, and *Eueides vibilia*). Different forward and reverse primers (supplementary table S2, Supplementary Material online) used in the study were designed against *BRh* and *LWRh* opsin sequences of *H. erato* (Zaccardi et al. 2006a), except for *D. moneta LWRh* which was obtained by rapid amplification of cDNA ends (RACE) PCR using gene-specific primers in combination with an adaptor primer (Marathon cDNA amplification kit; BD Biosciences). Lastly, we sequenced opsin cDNAs from the *H. melpomene* and *D. iulia* specimens used in the physiological experiments (see below) and included them in our analysis along with previously reported sequences from these species.

Phylogenetic Analysis

The *UVRh*, *BRh*, and *LWRh* opsin sequences were aligned in Mega 4.0 (Tamura et al. 2007), individually along with other members of each gene family downloaded from GenBank (see supplementary table S1, Supplementary Material online). A total of 1,134, 1,155, and 1,143 nucleotide characters were used in the phylogenetic reconstruction of the *UVRh*, *BRh*, and *LWRh* gene trees. For maximum likelihood analysis, the best-fit DNA substitution model was identified by running Modeltest (Posada and Crandall 1998) using the Akaike information criterion. Estimates of the gamma shape parameter and proportion of invariant sites were then used in the program PHYML (Guindon and Gascuel 2003) to obtain the 500 bootstrap replicates.

Branch-Site Test of Selection

Branch-site tests of selection are phylogeny-based tests that require the a priori identification of a foreground branch (indicated by a star in fig. 1*A*) that is hypothesized to be evolving at a different rate than the background branches in the rest of the tree. Unlike site models such as M1a or M2a (see p. 274 in Yang 2006) or branch models (Yang 1998), branch-site models permit the nonsynonymous–synonymous substitution ratio, ω, to vary both among sites and branches (Zhang et al. 2005). As in our prior study (Briscoe et al. 2010a), we specified the branch leading to the *Heliconius UVRh2* gene as the foreground branch and then proceeded to test the hypothesis, using a likelihood ratio test (LRT), that a branch-site model A which included two additional classes of sites with $\omega > 1$, indicating positive selection, was superior to a null model A where $\omega = 1$ for these two classes of site (Zhang et al. 2005). Both models contain other site classes in which $\omega = 1$ or was permitted to vary between 0 and 1. Codon frequencies were estimated based on the actual nucleotide frequencies at each of the three codon positions. We included all polymorphic/ambiguity sites in the analysis because we used a proofreading DNA *Taq* polymerase to obtain these sequences, and in most cases, these sites represent allelic variation present in the individual butterflies sequenced. We also used the Bayes empirical Bayes (BEB) method (Yang et al. 2005) as implemented in PAML 4.1 to identify the positively selected sites along this branch.

For the *BRh* and *LWRh* gene trees, we tested the hypothesis that the foreground branch leading to the *Heliconius* clade underwent positive selection concomitantly with the episode of positive selection detected along the branch leading to the *UVRh2* clade (see branches indicated by stars in fig. 1*B* and *C*). We did not test other branches in those trees for evidence of positive selection.

Small-Sample Method

The SSM was originally proposed to be appropriate for tests of both positive selection and episodic evolution when both the numbers of synonymous and nonsynonymous substitutions along a branch of interest were less than 10 (Zhang et al. 1997). The seminal paper on this topic (Zhang et al. 1997) used the primate lysozyme data of Messier and Stewart (1997) as an example. To test for positive selection along the branch leading to *UVRh2*, we first used maximum parsimony as implemented in Mesquite 2.72 (Maddison WP and Maddison DR 2009) to reconstruct ancestral sequences along each of the nodes shown in figure 1. This procedure seems justified because when we also performed empirical Bayesian reconstruction of ancestral sequences in PAML the accuracy (posterior probability) of the inferred ancestral sequences was over 99% on average. We then imported the ancestral sequences into MEGA (Tamura et al. 2007), excluded codon sites with gaps, and estimated the transition/transversion ratio (R) from the observed data using the maximum composite likelihood method considering all sequences, *UVRh2* sequences only, and *UVRh1* sequences only. Because the rate of transitional nucleotide changes was higher than transversional nucleotide changes, we selected the modified Nei–Gojobori method (Zhang et al. 1998) in MEGA to produce less biased estimates of the expected and observed numbers of nonsynonymous and synonymous differences between sequences for the branch leading to *UVRh2* using R as a parameter in the model. Fisher's exact test was calculated and P values smaller than 0.05 were considered significant at the 5% level.

To test for episodic evolution (Messier and Stewart 1997), that is, when positive selection is followed by

→

GTR+ Γ + I model with gamma shape parameters = 2.128, 1.4712, and 0.9591 and proportion of invariant sites = 0.495, 0.465, and 0.510. All codon positions were used in the reconstruction, and the reliability of the tree was tested using 500 maximum likelihood bootstrap replicates. Bar corresponds to the number of substitutions/site. Stars indicate foreground branches leading to clades specified as having a branch and site-specific rate of nucleotide substitution that is distinct from background branches in the branch-site test of selection shown in table 2. The dagger indicates sequences from the specimens used for epi-microspectrophotometry and optophysiology shown in figures 2 and 3. Bold indicates new sequences. λ_{max} data for *Speyeria* are from *Speyeria leto*.

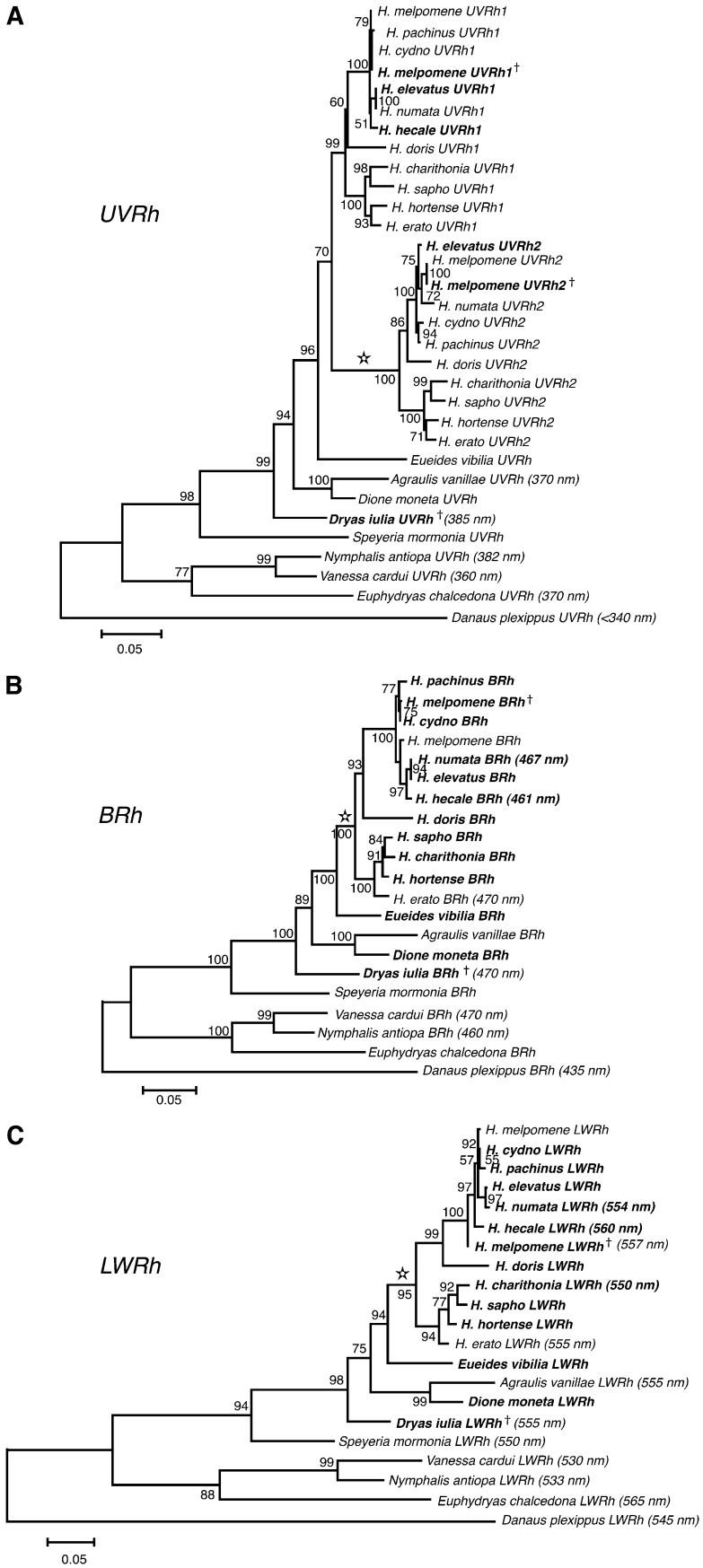

FIG. 1. Gene trees of opsins from Heliconiinae and outgroup nymphalid taxa made from full-length coding sequences. Trees of the (*A*) *UVRh*, (*B*) *BRh*, and (C) *LWRh* opsins shown are based upon maximum likelihood analysis of, respectively, 1,134, 1,155, and 1,143 bp using

negative selection, we first mapped the numbers of synonymous and nonsynonymous substitutions that occurred along all branches of the tree. We then compared the numbers of synonymous and nonsynonymous substitutions occurring along the branch leading to *UVRh2*, the positively selected branch, with the numbers of synonymous and nonsynonymous substitutions along all descendant branches using Fisher's Exact test.

Quantifying Phenotypic Variation

To compare the results of the molecular evolutionary analysis against phenotypic variation associated with these individual opsin sequences, we performed one or more of three distinct in vivo methods for estimating absorption spectra of the corresponding rhodopsin. Which method is suitable, or best, depends on the size of eye, the presence or absence of photostable lateral filtering pigments, the overall density of rhodopsin, and the level of stray light.

Epi-microspectrophotometry works best for obtaining partial bleaches of LWRh rhodopsin because substantial photo-conversion to metarhodopsin can be created with no conversion of UVRh and BRh rhodopsins (Bernard 1983; Frentiu, Bernard, Sison-Mangus, et al. 2007). Other necessary conditions are no lateral filtering pigments and low stray light (Briscoe and Bernard 2005). Retinal densitometry works best for estimating absorbance spectra of BRh and UVRh rhodopsins, if the measured ommatidia contain no lateral filtering pigments, stray light is low, and the tapetal reflectance spectrum is flat from the UV out to 600 nm or so (Bernard and Remington 1991; Briscoe et al. 2003, 2010a). Stray light is an experimental problem in large eyes, at wavelengths for which the round-trip density of rhodopsins and photoproducts in a rhabdom is 3 or more. In that case, so little light remains to be measured as eyeshine that it becomes similar to the intensity of residual reflections from the cornea and primary and secondary pigment cells, and diffuse reflections from elements of the optical train. Optophysiology measures action spectra of sensitized pupillary responses, which can produce estimates of the absorbance spectrum of LWRh rhodopsin in receptors driving the pupillary responses (Bernard and Wehner 1980; Bernard 1982). This method is suitable even for large eyes, high stray light, and ommatidia that contain lateral filtering pigment. When possible, an eye was studied with more than one method to increase confidence in our spectral characterizations.

We performed these experiments on seven species of heliconiine butterflies (see below) and compared λ_{max} estimates against newly calculated standard errors (SEs), 95% confidence intervals (CIs), and standard deviations (SDs) for previously reported experiments (Briscoe and Bernard 2005; Frentiu, Bernard, Sison-Mangus, et al. 2007; Briscoe et al. 2010). In some instances, for example, *H. erato* LWRh, we report new experimental results using experimental approaches complementary to the methods used in our prior reports. We note that our inferences regarding which opsin sequence corresponds to which rhodopsin absorbance spectrum is based on our prior comparative in situ hybridization studies of opsin mRNA expression in the retinas of *Vanessa cardui* (Briscoe et al. 2003), *Danaus plexippus* (Sauman et al. 2005), and *H. erato* (Zaccardi et al. 2006a, 2006b). The only point of ambiguity is which of the *Heliconius* UV opsins correspond to which of the identified UV rhodopsins due to cross-hybridization of their riboprobes (Zaccardi et al. 2006b).

Epi-microspectrophotometry

Absorption spectra can be measured directly from eyes of completely intact butterflies (Briscoe et al. 2003; Briscoe and Bernard 2005; Frentiu, Bernard, Sison-Mangus, et al. 2007). We used an epi-microspectrophotometer (epi-MSP) to measure eyeshine reflectance spectra, photo-convert the LWRh rhodopsin to its metarhodopsin photoproduct, and monitor the dark processes of metarhodopsin decay and rhodopsin recovery. Difference spectra were analyzed by nonlinear least-squares regression to Bernard's polynomial template for rhodopsin (Palacios et al. 1996) to estimate the absorbance spectrum of LWRh rhodopsin and its wavelength for maximal absorbance, λ_{max}.

Speyeria leto

The epi-MSP was set on a medioventral region of the female eye using 675 nm light, allowed to dark-adapt for 72 min, then treated with 10 min of intense 2 s/60 s flashes from a 45-watt halogen lamp filtered by Schott RG630. After 17 min, a photoproduct-free difference spectrum for partial bleach of LWRh rhodopsin was measured. On the following day, an optophysiological spectral sensitivity function was also measured from this same individual, described below.

Retinal Densitometry

To estimate absorbance spectra for the other spectral classes of rhodopsin, reflectance spectra were analyzed densitometrically using a stripping procedure first described in Briscoe et al. (2003). It exploits the fact that butterfly tapetal reflectors have constant reflectance from the UV out to a cutoff wavelength greater than 600 nm, beyond which tapetal reflectance decreases. Results for *H. erato* and *D. iulia* using this densitometric analysis were presented in Briscoe et al. (2010a). Results for additional species are present below.

Heliconius hecale

The epi-MSP was set on the darkly pigmented dorsal region of the eye using dim red light filtered by Schott RG665, then allowed to dark-adapt for 108 min after which a photoproduct-free reflectance spectrum was measured. Densitometric analysis of that reflectance spectrum produced λ_{max} estimates, R560, R465, and R398, that are consistent with three of the four visual pigments previously described in *H. erato*. There were also enough data points in the UV to be consistent with the presence of the fourth visual pigment, R355, in the *H. hecale* eye, but there were not enough to do the following statistical analyses performed for the other three rhodopsins to produce SEs, 95% CIs, and SDs. To produce these for the blue rhodopsin, the abovementioned λ_{max} estimates were used to create a least-squares fit by

stripping from the original reflectance spectrum the contributions from R355, R398, and R560, leaving a residual dominated by the blue rhodopsin. The normalized least-squares fit to the residual, restricted to wavelengths 390–650 nm, for which the tapetal reflectance is high and constant, was 464 ± 2 nm. Returning to the original reflectance spectrum and stripping contributions from R355, R464, and R560 leaves a residual fit by 396 ± 1 nm. Returning to the original spectrum and stripping R355, R396, and R464 creates a residual fit by: 560 ± 0.3 nm that compares favorably to the partial bleach 560 ± 1 nm published earlier (Frentiu, Bernard, Sison-Mangus, et al. 2007).

Nymphalis antiopa

After treating a medio-equatorial region of the eye with 36 min of intense 0.5 sec/20 sec flashes from a 45 watt halogen lamp filtered by Schott OG590, reflectance spectra were measured every 15 min to follow decay of metarhodopsin, ensuring that after 130 min the measured reflectance spectrum was free of photoproducts. Densitometric analysis of that reflectance spectrum produced the following initial λ_{max} estimates for the three visual pigments: R380, R460, and R533. As above, to calculate SEs, 95% CIs, and SDs, we performed a stripping procedure as follows. Stripping R380 and R533 created a residual fit by: 460 ± 1 nm. Stripping from the original spectrum, R460 and R533 created a residual fit by: 382 ± 1 nm. Stripping R380 and R460 from the original spectrum left a residual fit by: 533 ± 1 nm, which compares favorably to 533 ± 1 nm of the partial bleach published previously (Briscoe and Bernard 2005).

Agraulis vanillae

The epi-MSP was set on a patch of dorsal ommatidia having blue eyeshine lacking lateral red filtering pigments, treated with 15 h of intense 1 s/60 s flashes filtered by Schott OG590, then allowed to dark-adapt for 31 min after which a reflectance spectrum was measured. From a partial bleach published earlier (Frentiu, Bernard, Sison-Mangus, et al. 2007), we know that the LWRh rhodopsin is R555. To estimate the λ_{max} of the UVRh rhodopsin, we stripped R555 from the reflectance spectrum and performed a least squares fit.

Euphydryas chalcedona

The epi-MSP was set on a patch of dorsal ommatidia and allowed to dark-adapt for 120 min. The measured reflectance spectrum revealed only LWRh and UVRh rhodopsins. From a partial bleach published earlier (Frentiu, Bernard, Sison-Mangus, et al. 2007), we know the LWRh rhodopsin is R565. We therefore stripped R565 from the measured reflectance spectrum to produce the λ_{max} estimate of the UVRh rhodopsin.

Optophysiology

Butterfly photoreceptor cells contain intracellular granules that move centripetally in response to bright illumination and bleed light from the rhabdom by scattering and absorption, creating an effective pupillary response observable as a decrease in eyeshine reflectance (Stavenga et al. 1977). This intracellular pigment migration is mediated exclusively by photoisomerization of the rhodopsin contained within that same cell's rhabdomere. Thus, the pigment granules can be used as an optically measured, intracellular probe of physiological responses to light from that cell, measurable in a double-beam epi-MSP. A long-wavelength measuring beam (e.g., filtered by Schott RG695) monitors continuously the reflectance of eyeshine. A stimulating beam delivers monochromatic flashes that evoke pupillary responses. At each wavelength, the flash intensity is adjusted to produce a criterion decrease in reflectance. Wavelength sequence is randomized. This is a particularly good method for estimating λ_{max} of LWRh rhodopsin because the long-wavelength tail of the log-sensitivity function decreases linearly.

Heliconius erato

To produce an estimate of the LWRh λ_{max}, we used a steady measuring beam filtered by a Ditric 700-nm interference filter and a 2.0 optical density (OD) neutral density filter. Stimuli were 3 s monochromatic flashes separated by 30-s dark periods. Using randomized sequence of wavelengths every 10 nm between 460 and 670 nm, the quantum flux was adjusted to achieve a 10% criterion response at each wavelength. The results of two separate experiments are reported below.

Heliconius melpomene

A similar experiment with *H. melpomene* was used to estimate the LWRh λ_{max} by using filters Ditric 710 nm + 0.7 OD, 3 s/50 s flashes, and 6% criterion responses, from the eye's dorsal pole.

Agraulis vanillae

The measuring filters used to estimate LWRh λ_{max} were Hoya IR76 + 0.6 OD with 30 s/300 s flashes and 7% criterion responses from the medio-equatorial eye region.

Speyeria leto

For the same female described in the epi-microspectrophotometry experiment above, measuring filters used to estimate LWRh λ_{max} were Schott RG665 + 0.6 OD with 5 s/120 s flashes and 8% criterion responses from the medioventral eye region.

Results and Discussion

Molecular and Physiological Evidence for Three Rhodopsins in the Eyes of Heliconius Relatives

Previously, we cloned *UVRh1* and *UVRh2* from nine *Heliconius* species (Briscoe et al. 2010a), *BRh* from two *Heliconius* species (Pohl et al. 2009), and partial genomic DNA sequences of *LWRh* from seven *Heliconius* species (Hsu et al. 2001). We now report the isolation of full-length *UVRh1* and *UVRh2* cDNAs from the eyes of a tenth species, *H. elevatus*, and *UVRh1* from an eleventh species, *H. hecale*.

We also isolated opsin mRNAs from the *H. melpomene* and *D. iulia* specimens studied physiologically (see below), and we isolated full-length *BRh* and *LWRh* cDNAs, which have not been previously reported, from ten *Heliconius*

species, and also from *E. vibilia*, *D. iulia*, and *D. moneta* (supplementary table S1 and fig. S1, Supplementary Material online). The 32 newly isolated cDNAs (GenBank accession nos. GU324674–GU324705) encoded opsins that were 376–378 (UVRh), 380–381 (BRh), and 380 (LWRh) amino acids in length.

The results of our cDNA screens uphold the view that at least ten *Heliconius* species, representing 23% of recognized species, have eyes that express four opsin-encoding mRNAs, whereas all heliconiine outgroup taxa examined so far, *E. vibilia*, *A. vanillae*, *D. moneta*, *D. iulia*, and *S. mormonia*, have eyes that express only three opsin-encoding mRNAs. The maximum likelihood gene trees reconstructed from coding sequence of each of the three major spectral classes of rhodopsins produced identical results for the branching order of all taxa outside the *Heliconius* clade (fig. 1). The bootstrap support for these outgroup taxa was also reasonably good, ranging from 75 to 100% for all outgroup nodes in each of the three gene trees. Overall, the phylogenies we obtained individually with the opsins were concordant with other recent phylogenies of these genera obtained using independent mitochondrial and nuclear DNA molecular markers (e.g., Beltran et al. 2007; Mallet et al. 2007). As is evident from the branching pattern of the UV opsin gene tree, the gene duplication giving rise to *UVRh1* and *UVRh2* arose sometime after the split between the genus *Heliconius* and *Eueides*, along the lineage leading to *Heliconius*, confirming our earlier findings (Briscoe et al. 2010a). Although divergence time estimates do not currently exist for the *Heliconius*–*Eueides* split, which might provide an estimate of when the duplicate UV opsins arose, divergence between the *H. erato* and *H. melpomene* lineages has been estimated to have occurred between 14 and 26 Ma (Pohl et al. 2009), so the UV opsin gene duplication presumably arose sometime before this.

There have been approximately 35 species of butterfly whose visual pigments have been previously studied using epi-microspectrophotometry, intracellular recordings, or electroretinograms (see references in table 1 in Frentiu and Briscoe 2008). For anatomical and technical reasons mentioned above, including their high abundance compared with other visual pigments, the long-wavelength–sensitive visual pigments are easier to study than the other spectral classes and tend to be the only class of visual pigment for which spectral data are available for a given species. For each of the previously studied 35 species, the wavelength of peak absorbance, λ_{max}, of the long-wavelength–sensitive rhodopsins has been characterized. By contrast, the blue- and ultraviolet-sensitive rhodopsins have been characterized from only 14 of these species. Our study contributes spectral data for two new long-wavelength–sensitive rhodopsins (5% of all LWRh spectral data for individual species), two new blue-sensitive rhodopsins (13% of all BRh data), and four new ultraviolet-sensitive rhodopsins (22% of all UVRh data). The lack of spectral data for the BRh and UVRh rhodopsins of butterflies has hampered the examination of an important question in sensory ecology: when there is selection for the tuning of one visual pigment is there selection for tuning of the other visual pigments? There is no straightforward way of predicting this from sequence data alone—functional data as we report below are needed.

Our physiological experiments allowed us to obtain λ_{max} values including 95% CIs and SDs for previously unreported rhodopsins of *H. hecale*, *H. melpomene*, *A. vanillae*, *S. leto*, *N. antiopa*, and *E. chalcedona* (table 1 and figs 2 and 3). Also added to figure 2 are results for the visual pigments of *D. iulia* (reported previously in Briscoe et al. 2010a) in a form that makes them comparable to the data shown here. Together with previous experimental results reporting the λ_{max} values of the long-wavelength–absorbing rhodopsins of these same species (Briscoe and Bernard 2005; Frentiu, Bernard, Sison-Mangus, et al. 2007), we found physiological evidence of three rhodopsins in the eyes of the four outgroup species mentioned above, as well as the outgroup nymphalid *V. cardui* (Briscoe et al. 2003). With these physiological, molecular, and phylogenetic data, we were able to examine the possibility of coordinated tuning of different spectral classes of rhodopsins (see below).

Evidence for Coordinate Tuning of Both UVRh1 and UVRh2

Together with the results of previous studies (Briscoe et al. 2003; Stalleicken et al. 2006; Briscoe et al. 2010a), the UV-absorbing rhodopsins in the studied species ranged in their wavelength of peak absorbance from <340–399 nm. Character mapping of the λ_{max} values of the UV rhodopsins on the UV opsin gene tree, where the available evidence suggests a one-to-one correspondence between the opsin sequence shown and the rhodopsin absorbance spectrum given in parentheses, indicates that the two species that are in genera closely related to *Heliconius*, *D. iulia*, and *A. vanillae*, both have single UV rhodopsins with λ_{max} values (385 and 370 nm) that are intermediate in value between either of the classes of duplicated UV rhodopsin in *Heliconius*: λ_{max} = 349–355 nm or λ_{max} = 396–399 nm (fig. 1). The new spectral data from outgroup taxa *N. antiopa* (λ_{max} = 382 nm) and *E. chalcedona* (λ_{max} = 370 nm) also supports this conclusion. Collectively, the data would seem to suggest that both *Heliconius* UV rhodopsins underwent spectral shifts because they shared a hypothetical common ancestor with *A. vanillae* and *D. iulia*. Obtaining λ_{max} estimates for the UV-absorbing rhodopsins of *E. vibilia* or *D. moneta* would help clarify the origins of this apparent spectral shift.

The UV rhodopsins with the shortest wavelength of peak absorbance among those in the present study are the UV rhodopsin of *H. erato* and *H. numata* with λ_{max} = 349–355 nm (Briscoe et al. 2010a) and the UV rhodopsin of the most basal nymphalid, *D. plexippus*, whose UV-sensitive photoreceptor was estimated to have a peak sensitivity <340 nm (Stalleicken et al. 2006). The largest magnitude shift in λ_{max} over the entire nymphalid UV opsin tree was therefore observed between the two spectral classes of *Heliconius* UV rhodopsins, 349–355 nm and

Table 1. Absorbance Spectrum Maxima (λ_{max}) Values of Rhodopsins.

Subfamily	Species	Method	λ_{max} ± SE (nm)	95% CI	SD (log units)	Opsin Gene
Nymphalinae	*Euphydryas chalcedona*	Densitometry	370 ± 1	368–372	0.03	*UVRh*
		epi-MSP	565 ± 1[a]	564–566	0.02	*LWRh*
Nymphalinae	*Nymphalis antiopa*	Densitometry	382 ± 1	380–384	0.03	*UVRh*
		Densitometry	460 ± 1	458–462	0.04	*BRh*
		epi-MSP	533 ± 1[b]	532–535	0.03	*LWRh*
Heliconiinae	*Speyeria leto*	epi-MSP	552 ± 1	550–555	0.06	*LWRh*
		Optophysiology	551 ± 0.5	549–552	0.03	
Heliconiinae	*Agraulis vanillae*	Densitometry	370 ± 1	368–373	0.02	*UVRh*
		epi-MSP	555 ± 0.5[a]	554–556	0.01	*LWRh*
Heliconiinae	*Dryas iulia*	Densitometry	385 ± 1[c]	383–387	0.04	*UVRh*
			470 ± 3[c]	464–475	0.13	*BRh*
			556 ± 1[c]	553–558	0.05	*LWRh*
Heliconiinae	*Heliconius hecale*	Densitometry	396 ± 1	394–398	0.03	?
		Densitometry	464 ± 2	461–468	0.09	*BRh*
		epi-MSP	560 ± 1[a]	559–561	0.01	*LWRh*
Heliconiinae	*H. erato*	Optophysiology	555 ± 0.5	554–556	0.04	*LWRh*
			555 ± 1	553–557	0.07	
Heliconiinae	*H. melpomene*	Optophysiology	557 ± 0.8	555–559	0.03	*LWRh*

[a] Normalized absorbance spectrum presented in Frentiu, Bernard, Sison-Mangus, et al. (2007). SEs, 95% CIs, and SDs are newly presented here.
[b] Normalized absorbance spectrum presented in Briscoe and Bernard (2005). SEs, 95% CIs, and SDs are newly presented here.
[c] Reflectance spectrum data presented in Briscoe et al. (2010a).

396–398 nm, respectively. Putting the physiological data for the UV-sensitive rhodopsins into a phylogenetic context therefore highlights the rarity of the spectral tuning event observed in *Heliconius*.

Positive Selection and Episodic Evolution of Heliconius UVRh2

As we had found with our prior study (Briscoe et al. 2010a), the branch-site test of selection using the phylogeny that included new sequences from *H. elevatus*, *H. melpomene*, and *H. hecale* revealed positive selection along the branch leading to the *UVRh2* clade (fig. 1*A*). Because the hypothesis of neutral evolution was rejected (LRT = $2\Delta\ell = 10.26$, degrees of freedom [df] = 1, $P = 0.001$), we used a BEB approach to identify positively selected sites at the 95% or above level. In total 26 positively selected sites along the branch leading to *UVRh2* were identified by the method (table 2), two fewer sites than were identified using a smaller data set (Briscoe et al. 2010a) because their BEB probabilities dropped below 95%. A diagram of the location of the BEB-identified positively selected sites is shown in figure S2 (Supplementary Material online).

A recent study of dim-light rhodopsins in fish has indicated that naive empirical Bayes (NEB) or BEB estimates of positively selected sites can sometimes produce false positives, especially when closely related species are compared (Yokoyama et al. 2008). Interestingly, the predicted positively selected sites completely disappeared when more distantly related sequences were included in the analysis. The explanation offered for this behavior of the statistical test was that even under neutral or even slightly deleterious selection, random mutation of a sequence initially produces approximately 70% nonsynonymous changes

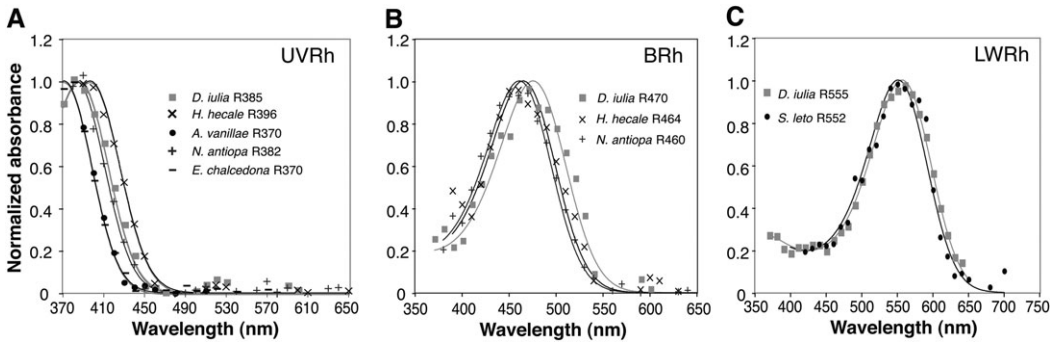

Fig. 2. Absorbance spectra of UV, blue, and long-wavelength–absorbing rhodopsins in the eyes of representative species from three heliconiine genera based on epi-microspectrophotometric and retinal densitometric measurements of partial bleaches. Idealized rhodopsin spectra (solid curves) based on the Bernard template (Palacios et al. 1996). (*A*) Absorbance spectra of UV-absorbing rhodopsin of *D. iulia* (λ_{max} = 385 ± 1 nm), *Heliconius hecale* (λ_{max} = 396 ± 1 nm), *Agraulis vanillae* (λ_{max} = 370 ± 1 nm), *Nymphalis antiopa* (λ_{max} = 382 ± 1 nm), and *Euphydryas chalcedona* (λ_{max} = 370 ± 1 nm). (*B*) Absorbance spectra of blue-absorbing rhodopsin of *D. iulia* (λ_{max} = 470 ± 3 nm), *H. hecale* (λ_{max} = 464 ± 2 nm), and *N. antiopa* (λ_{max} = 460 ± 1 nm). (*C*) Absorbance spectra of long-wavelength–absorbing rhodopsin of *D. iulia* (λ_{max} = 556 ± 1 nm) and *Speyeria leto* (λ_{max} = 552 ± 1 nm); 95% CIs and SDs are given in table 1.

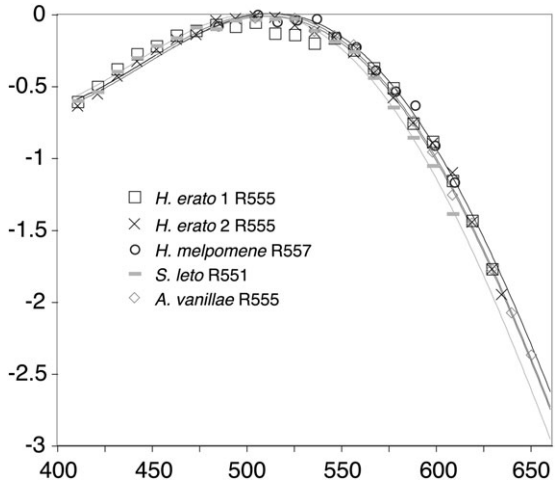

FIG. 3. Action spectrum of long-wavelength–absorbing rhodopsins in the eyes of *Heliconius erato*, *H. melpomene*, *Agraulis vanillae*, and *Speyeria leto* based on optophysiology. Idealized log sensitivity (solid curves) based on the Bernard rhodopsin template. Log sensitivity of LWRh of *H. erato* from two experiments (squares, $\lambda_{max} = 555 \pm 1$ nm/crosses, 555 ± 0.5 nm), *H. melpomene* (circles, $\lambda_{max} = 557 \pm 1$ nm), *A. vanillae* (diamonds, $\lambda_{max} = 555 \pm 0.5$ nm), and *S. leto* (dashes, $\lambda_{max} = 551 \pm 0.5$ nm); 95% CIs and SDs are given in table 1.

compared with only 30% synonymous changes. However, as time increases, the number of synonymous changes will eventually accumulate faster than nonsynonymous changes. The differential rates of nonsynonymous versus synonymous substitutions at different points in evolution may explain the false-positive rate.

Importantly for our current study, the hypothesis that random mutations will initially produce more nonsynonymous than synonymous substitutions along the branch leading to *UVRh2* can be tested using the small-sample method and Fisher's exact test (Zhang et al. 1997; Briscoe et al. 2010b). As we describe below, the small-sample method upholds our initial finding of positive selection of *UVRh2* using the BSM. The issue of whether sites that are subsequently identified as being positively selected were indeed selected for rhodopsin spectral tuning is another matter (see below).

Another recent study (Nozawa et al. 2009) has similarly been critical of site prediction methods and models such as M8, REL, FEL, and DEPS and also uses vertebrate rhodopsin data sets to test these methods. It is difficult to directly compare the results of the articles of Yokoyama et al. (2008) and Nozawa et al. (2009) to our results because the specific PAML models used in their studies are site models (M2a, M8) and are somewhat different than the branch-site model used in our study. In site models, codons in an alignment are binned into different classes of site, where $\omega < 1$, $\omega = 1$, and $\omega > 1$, and the rate of evolution over all branches of the tree are assumed to be the same, whereas branch-site models permit both site-specific and branch-specific differences in the rate of evolution. Nozawa et al. (2009) also pool both NEB and BEB results together when assessing the false-positive rate. The data sets are also different—mostly orthologous genes in the articles of Yokoyama et al. (2008) and Nozawa et al. (2009) compared with paralogous genes here—but the underlying principles are presumably the same. In addition, as indicated in the supplementary tables S6–S8 of Yokoyama et al. (2008), ~50% of the sites that tend to be falsely identified as positively selected using NEB or BEB methods are those which have three to four different types of tolerated amino acids. In the examples from our own data set, this is not the case, except for sites 225 and 227 (table 2).

Our own view is that statistical methods for detecting positive selection are useful starting points for identifying functionally interesting parts of the genome for further characterization (Briscoe 2010b). Independent sources of evidence, including comparative physiological data as we have reported in the present study, structural modeling, and the biochemical relevance of identified substitutions are all important considerations when sizing-up the potential significance of identified sites for further functional study. Below, we use these independent criteria to discuss the sites we consider to be most promising for experimental work elucidating the molecular basis of butterfly UV rhodopsin spectral tuning. We note that in the discussion below and in the critical papers cited above, only the relevance of the identified positively selected sites to rhodopsin spectral tuning is considered. It is highly likely that some of the sites that are deemed irrelevant to rhodopsin spectral tuning by the above studies may have been in fact positively selected for other protein functions, such as metarhodopsin spectral tuning and protein stability. Further experimental work on visual pigment photoproducts and their associated stabilities are needed to rule out that possibility.

In light of these considerations, we do not think that all the BEB-identified sites are in fact positively selected, for example, sites 190 and 321 are valine to isoleucine substitutions, which are probably neutral changes. We do think that some of them are worthy candidates for functional testing using site-directed mutagenesis. For example, homology modeling of the UVRh rhodopsins of *H. erato* indicates two of these sites 179 and 289 correspond to experimentally determined spectral tuning sites 180 and 277 in the human red cone pigment numbering system (Asenjo et al. 1994) (supplementary table S3, Supplementary Material online). Most notably, the two *Heliconius* visual pigments differ in having amino acid changes A180T and F277Y at these sites. In site-directed mutagenesis experiments, amino acid changes A180S and F277Y increased λ_{max} values of human green pigment by ~7 and 10 nm, respectively, and the effects of these amino acid substitutions on λ_{max} were approximately additive (Asenjo et al. 1994). These two sites have also extensively been examined by site-directed mutagenesis of ancestral vertebrate red and green cone pigment genes and their effects on spectral tuning have been upheld (Yokoyama et al. 2008).

Interestingly, in the study of Nozawa et al. (2009), amino acid sites 180 and 285 in human red cone pigment are two sites (out of six total) that were correctly identified as being positively selected among the primate middle- and long-

Table 2. Log Likelihood Values and Parameter Estimates for the *UVRh2* Opsin Branch-Site Test of Selection.

Branch	Model	ℓ	Site Class	Proportion (ω)	Background (ω)	Foreground (ω)	Positively Selected Substitutions
a	**A**	**−7056.07**	**0**	**0.74737**	**0.03055**	**0.03055**	**D35E, A37E, L60M, F77Y, T121I, M132V[a], A145L, M171L, A179T[b], M185L, N189R, V190I, S202A, T204S, V218T, C224F, S225T/A[b], V/L227A, F228I, M230L, I234M, F236Y, F289Y[b], T312S, V321I, A361V**
			1	**0.05797**	**1.00000**	**1.00000**	
			2a	**0.18065**	**0.03055**	**7.81830**	
			2b	**0.01401**	**1.00000**	**7.81830**	
	Null	**−7061.21**	**0**	**0.39038**	**0.03044**	**0.03044**	
			1	**0.03052**	**1.00000**	**1.00000**	
			2a	**0.53712**	**0.03044**	**1.00000**	
			2b	**0.04199**	**1.00000**	**1.00000**	

NOTE.—BEB-identified positively selected sites are inferred at $P = 95\%$ with those reaching 99% shown in bold. For *UVRh*, the LRT $= 2\Delta\ell = 10.26$, df $= 1$, $P = 0.001$.

[a] Corresponds to bovine rhodopsin amino acid residue 116.

[b] Homologous to human red cone pigment amino acid residues 180, 227, and 277.

wavelength–sensitive opsins (green- and red-sensitive cone pigments) by the M8 model and BEB method. Even though a significant number of other sites were identified as being positively selected where experimental evidence suggested no effect on spectral tuning, it is worthwhile to mention that sites 180 and 285 are two of three amino acid sites that have the largest impact (7 and 16 nm, respectively) on spectral tuning of the primate middle- and long-wavelength–sensitive visual pigments (Yokoyama and Radlwimmer 1998). Probably the identification of a few sites that are relevant for spectral tuning is the best we can hope for from statistical methods alone, in the absence of theory from quantum chemists and direct experimental data.

Intriguingly, we did identify one amino acid site containing an identical substitution also found in avian ultraviolet- and violet-sensitive visual pigments. Site 132 (corresponding to site 116 in bovine rhodopsin) contains M in UVRh1 and V in UVRh2 (supplementary table S3, Supplementary Material online). Introduction of a V116M mutation into pigeon short-wavelength–sensitive (SWS1) visual pigment resulted in an 8-nm blue shift, an effect that has been suggested to be due to conformational changes rather than direct interactions with the chromophore (Carvalho et al. 2007). Other sites near the chromophore, such as polymorphic site S225T/A (equivalent to 227 in human red cone pigment), harbor the class of substitution—a hydroxyl-bearing for a nonhydroxyl-bearing amino acid—that cause spectral tuning effects in other classes of vertebrate pigment. Mutations at site 225 in bovine rhodopsin (equivalent to H211F and H211C) reduce λ_{max} values by 3 and 5 nm, respectively (Nathans 1990). Also worth mentioning is the N189R substitution inferred at 95% probability, which involves the substitution of asparagine, a smaller uncharged residue with arginine, a much larger residue with a basic charge. This residue maps to the putative second extracellular loop domain, several sites within which affect spectral tuning of bovine rhodopsin (supplementary fig. S2, Supplementary Material online) (Palczewski et al. 2000). All these sites are probably worth exploring experimentally using site-directed mutagenesis. We also acknowledge the possibility that other sites not detected in the BEB analysis may be responsible, in part, for spectral tuning (see supplementary table S3, Supplementary Material online). For example, it is possible that epistatic substitutions which occurred along the branch or branches leading to the common ancestor of *UVRh1* and *UVRh2* may be critical for the spectral function of one or the other UV-absorbing rhodopsins as has been recently demonstrated in a fascinating study on the red fluorescent proteins in corals (Field and Matz 2010).

Are the sites identified as positively selected above that have been found to have functional effects in vertebrate rhodopsins likely to have an effect on spectral tuning of butterfly UVRh2? Quite possibly, as two separate studies have found that spectral tuning of different classes of *Drosophila* rhodopsin is mediated by at least two sites that were shown to be critical for spectral tuning of other vertebrate rhodopsins (see Salcedo et al. 2003, 2009).

Because *Heliconius UVRh1* and *UVRh2* are so closely related, we next mapped the parsimony-reconstructed numbers of synonymous (S) and nonsynonymous (NS) substitutions onto each branch of the UV opsin gene tree using transition/transversion ratio, $R = 1.4$ (all 32 sequences) or $R = 1.9$ (*UVRh2* only) (fig. 4). All counts were identical regardless of the R value. What is striking is that the only branch where NS > S is along the branch (*a*) leading to the *UVRh2* clade. For all other branches, the reverse relationship is shown, which is expected under neutral evolution or purifying selection.

The results of the SSM for detecting positive selection along branch *a* using Fisher's exact test was significant over all three estimates of the transition/transversion ratio (R) obtained from the observed sequences. P values ranged from 0.035 for $R = 1.4$ (all 32 sequences),to 0.027 for

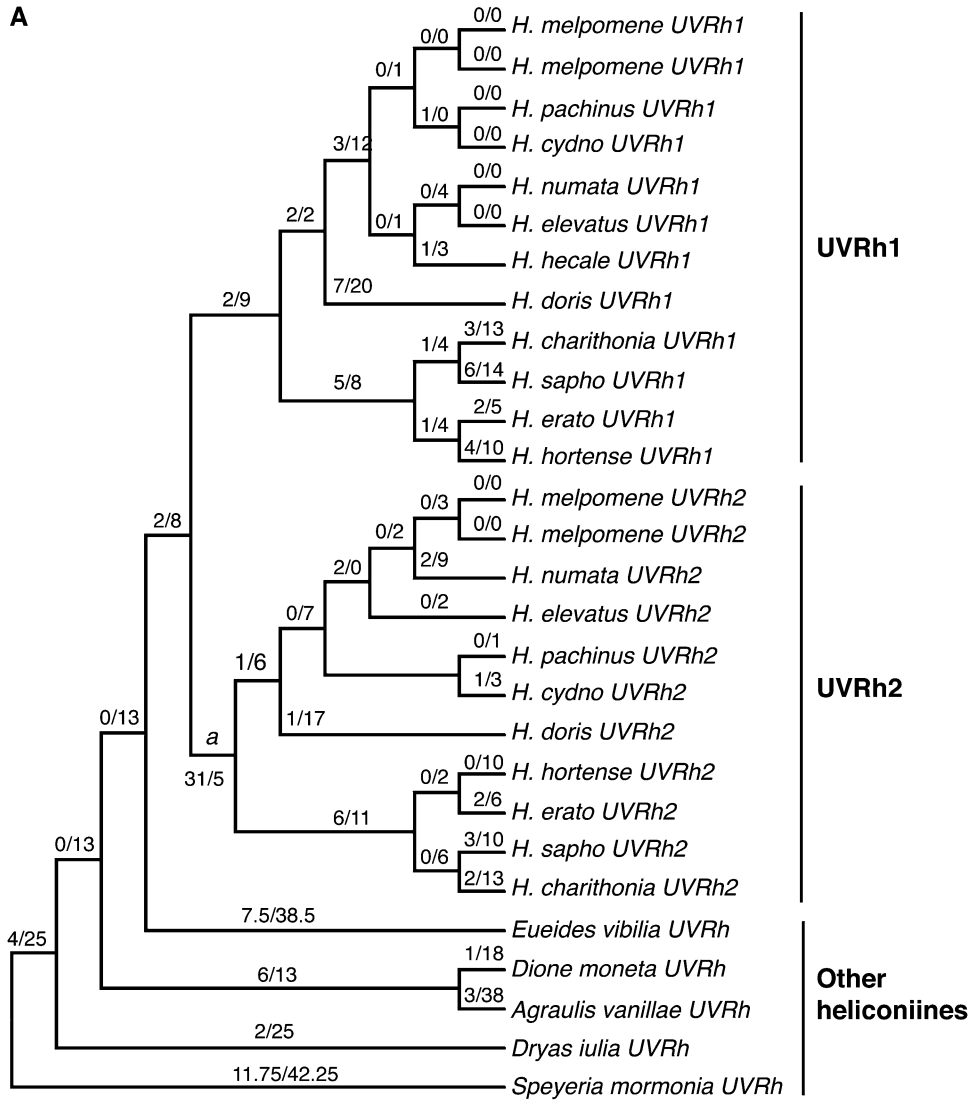

B

Test of episodic evolution

	Numbers of substitutions	
	NS	S
Branch *a*	31	5
Desc. lineages	21	109

$P = 7.76 \times 10^{-15}$

FIG. 4. Test of episodic evolution of *Heliconius* UVRh2 rhodopsins. (*A*) Numbers of synonymous (S) and nonsynonymous (NS) nucleotide substitutions per sequence for each branch of the phylogenetic tree of heliconiine UV opsin genes using a transition/transversion rate ratio, $R = 1.4$, and the modified Nei–Gojobori method. A total of 374 codons were included in the analysis. The ancestral nucleotide sequences at the interior nodes were inferred by the parsimony method (Fitch 1971). (*B*) Test of episodic evolution. *P* value shown was calculated according to Fisher's exact test.

$R = 1.9$ (all *UVRh1* sequences) and to 0.027 for $R = 1.9$ (all *UVRh2* sequences). We note that *P* values <0.05 are considered significant at the 5% level (Kumar et al. 2008). Because the SSM has been shown to be more conservative than the BSM in simulation studies (Nozawa et al. 2009), these results strengthen our prior detection of positive selection of *UVRh2* following gene duplication using the BSM (Briscoe et al. 2010a).

We note, in addition, that our result rules out the possibility that the acquisition of a new function by *UVRh2* proceeded by random fixation of neutral mutations which later resulted in a change in gene function when the environment or genetic background was altered, a process known as the Dykhuizen–Hartl effect (Dykhuizen and Hartl 1980). This is because under that scenario, the rate of nonsynonymous substitution along branch *a* will never exceed

the rate of synonymous substitution, whereas we found the opposite to be the case.

The test of episodic evolution, testing the hypothesis of positive selection along the branch leading to *UVRh2*, followed by purifying selection on all descendant branches, was highly significant ($P = 7.76 \times 10^{-15}$) (fig. 4*B*). By contrast, the same test conducted in parallel by examining all the substitutions along the branch leading to *UVRh1* and all descendant branches was not significant ($P = 0.83$). These complementary tests highlight the burst of adaptive amino acid changes leading to the evolution of *UVRh2*, in contrast to the more conservative mode of evolution on *UVRh1*.

We note that the null hypothesis of the SSM implemented in the tests for positive selection is hard to reject. Even other examples of genes where positive selection has been detected by one statistical method (e.g., primate lysozymes analyzed using a *t*-test) (Messier and Stewart 1997) has been rejected by the SSM (Zhang et al. 1997). The reasons for this, especially for vertebrate rhodopsins, have been explored elsewhere (Nozawa et al. 2009) and include the fact that adaptive variation may depend on a single amino acid substitution (Hoekstra et al. 2006), which these methods are not designed to detect. In the case of *UVRh2*, it would seem that many amino acid substitutions might have been required to produce a new spectrally distinct UV-absorbing rhodopsin. This may be because it requires higher energy photons to photoconvert UV rhodopsins compared with rhodopsins with absorption spectra in the visible range, and this may have required more extensive remodeling of the chromophore-binding pocket to accommodate as well as changes in sites away from the chromophore. There is also the possibility that like the SWS1 visual pigments in vertebrates, the mutations responsible for spectral tuning of the UV rhodopsins may be nonadditive in effect, and single substitutions may be much larger in effect due to changes in protonation of the Schiff base than are observed in the middle- and long-wavelength–sensitive visual pigments in vertebrates (Wilkie et al. 2000; Cowing et al. 2002; Fasick et al. 2002; Yokoyama et al. 2006; Carvalho et al. 2007).

Purifying Selection on BRh and LWRh

With one exception, all the studied blue-absorbing rhodopsins ranged in their wavelength of peak absorbance from 460 to 470 nm, suggesting that there was no major spectral tuning of the blue rhodopsin along the branch leading to the *Heliconius* BRh lineage. This exception, occurred at the base of the blue opsin phylogeny, in the blue photoreceptor of the monarch butterfly, *D. plexippus* (fig. 1), whose spectral sensitivity was estimated using intracellular recordings as $\lambda_{max} = 435$ nm (Stalleicken et al. 2006). It will be interesting to see whether any other butterflies in closely related genera such as *A. vanillae*, *E. vibilia*, or *D. moneta* have blue-absorbing rhodopsins in the 460- to 470-nm range we found in the other studied nymphalids. The sequence data so far suggest a conservative mode of evolution. That is to say, we found no evidence of positive selection along the branch leading from the hypothetical common ancestor of *Eueides* and *Heliconius*, and the *Heliconius* BRh clade (supplementary table S4, Supplementary Material online, LRT = 0).

The long-wavelength–absorbing rhodopsins over our entire data set ranged in their wavelength of peak absorbance from 530 to 560 nm (figs 1–3). Within the heliconiine subfamily, this value ranged from 550 to 560 nm with a similar range of values within the *Heliconius* genus. Character mapping of these λ_{max} values onto the *LWRh* phylogeny suggests that like the blue-absorbing rhodopsin, tuning of the long-wavelength–absorbing rhodopsin was unlikely to have occurred along the branch leading to the *Heliconius* genus. The results of our branch-site test of selection for the LWRh opsin are consistent with this ($2\Delta\ell = 1.54$, df = 1, $P = 0.215$) (supplementary table S4, Supplementary Material online). It will be interesting to see whether λ_{max} estimates for the LWRh rhodopsins of *E. vibilia* and *D. moneta* confirm this prediction.

Conclusions

In conclusion, we confirmed our prior findings of positive selection and report complimentary evidence of episodic evolution of the *Heliconius UVRh2* gene following duplication. Our new physiological data for the other spectral classes of visual pigment also indicate that spectral tuning of the *Heliconius* UV-absorbing rhodopsins did not at the same time impact spectral tuning of the *Heliconius* BRh or LWRh rhodopsins. In general, the evolution of λ_{max} of the BRh and LWRh spectral classes of rhodopsin appears to be conservative throughout most of the heliconiine subfamily, and both molecular and physiological data point to the same conclusions. We did, however, find evidence that the *Heliconius* UVRh1 and UVRh2 rhodopsins may have both shifted their spectral sensitivities because they shared a common ancestor with *A. vanillae*. This suggests potential compensatory evolution between the two copies—perhaps for the purpose of color vision in the context of species recognition. Visual models of how butterflies perceive yellow wing colors indicate that if *H. erato* uses UVRh1, UVRh2, and LWRh rhodopsins together for species recognition, it may have an advantage over other heliconiine butterflies lacking the UV opsin duplicate in discriminating wing color variation (Briscoe et al. 2010a). It will be interesting to see if site-directed mutagenesis validates the functional significance of the sites inferred to be positively selected that also contain structurally and biochemically relevant substitutions. Lastly, we note that although it may be impossible to ever infer the impact on *Heliconius* fitness of *UVRh2*, it is still possible to determine its current utility to the animals through behavioral tests (Sison-Mangus et al. 2008).

Supplementary Material

Supplementary tables S1–S4 and figures S1 and S2 are available at *Molecular Biology and Evolution* online (http://www.mbe.oxfordjournals.org/).

Acknowledgments

We thank Maita Kuvhenguhwa and Marilou P. Sison-Mangus for laboratory assistance and Robert Reed, Jorge Llorente-Bousquets, Larry Gilbert, Charles L. Remington, and Andrew Warren for providing butterfly tissue. This work was supported by National Science Foundation grant IOS-0819936.

References

Arikawa K, Wakakuwa M, Qiu X, Kurasawa M, Stavenga DG. 2005. Sexual dimorphism of short-wavelength photoreceptors in the small white butterfly, *Pieris rapae crucivora*. *J Neurosci*. 25:5935–5942.

Asenjo AB, Rim J, Oprian DD. 1994. Molecular determinants of human red/green color discrimination. *Neuron* 12:1131–1138.

Baxter SW, Nadeau NJ, Maroja LS, et al. (19 co-authors). 2010. Genomic hotspots for adaptation: the population genetics of Mullerian mimicry in the *Heliconius melpomene* clade. *PLoS Genet*. 6:e1000794.

Beltran M, Jiggins CD, Brower AVZ, Bermingham E, Mallet J. 2007. Do pollen feeding, pupal-mating and larval gregariousness have a single origin in *Heliconius* butterflies? Inferences from multilocus DNA sequence data. *Biol J Linn Soc*. 92:221–239.

Bernard GD. 1982. Non-invasive optical techniques for probing insect photoreceptors. *Methods Enzymol*. 81:752–759.

Bernard GD. 1983. Dark-processes following photoconversion of butterfly rhodopsins. *Biophys Struct Mech*. 9:277–286.

Bernard GD, Remington CD. 1991. Color vision in *Lycaena* butterflies—Spectral tuning of receptor arrays in relation to behavioral ecology. *Proc Natl Acad Sci U S A*. 88:2783–2787.

Bernard GD, Wehner R. 1980. Intracellular optical physiology of the bees eye. 1. Spectral sensitivity. *J Comp Physiol*. 137:193–203.

Briscoe AD. 1998. Molecular diversity of visual pigments in the butterfly *Papilio glaucus*. *Naturwissenschaften* 85:33–35.

Briscoe AD. 2008. Reconstructing the ancestral butterfly eye: focus on the opsins. *J Exp Biol*. 211:1805–1813.

Briscoe AD, Bernard GD. 2005. Eyeshine and spectral tuning of long wavelength-sensitive rhodopsins: no evidence for red-sensitive photoreceptors among five Nymphalini butterfly species. *J Exp Biol*. 208:687–696.

Briscoe AD, Bernard GD, Szeto AS, Nagy LM, White RH. 2003. Not all butterfly eyes are created equal: rhodopsin absorption spectra, molecular identification and localization of ultraviolet-, blue-, and green-sensitive rhodopsin-encoding mRNAs in the retina of *Vanessa cardui*. *J Comp Neurol*. 458:334–349.

Briscoe AD, Bybee SM, Bernard GD, Yuan F, Sison-Mangus MP, Reed RD, Warren AD, Llorente-Bousquets J, Chiao CC. 2010a. Positive selection of a duplicated ultraviolet-sensitive visual pigment coincides with wing pigment evolution in *Heliconius* butterflies. *Proc Natl Acad Sci U S A*. 107:3628–3633.

Briscoe AD, Bybee SM, Bernard GD, Yuan F, Sison-Mangus MP, Reed RD, Warren AD, Llorente-Bousquets J, Chiao CC. 2010b. Reply to Nozawa et al.: complementary statistical methods support positive selection of a duplicated UV opsin gene in *Heliconius*. *Proc Natl Acad Sci U S A*. 107:E97.

Carvalho LS, Cowing JA, Wilkie SE, Bowmaker JK, Hunt DM. 2007. The molecular evolution of avian ultraviolet- and violet-sensitive visual pigments. *Mol Biol Evol*. 24:1843–1852.

Counterman BA, Araujo-Perez F, Hines HM, et al. (18 co-authors). 2010. Genomic hotspots for adaptation: the population genetics of Mullerian mimicry in *Heliconius erato*. *PLoS Genet*. 6: e1000796.

Cowing JA, Poopalasundaram S, Wilkie SE, Robinson PR, Bowmaker JK, Hunt DM. 2002. The molecular mechanism for the spectral shifts between vertebrate ultraviolet- and violet-sensitive cone visual pigments. *Biochem J*. 367:129–135.

Dykhuizen D, Hartl DL. 1980. Selective neutrality of 6PGD allozymes in *Escherichia coli* and the effects on genetic background. *Genetics* 96:801–817.

Fasick JI, Applebury ML, Oprian DD. 2002. Spectral tuning in the mammalian short-wavelength sensitive cone pigments. *Biochemistry* 41:6860–6865.

Field SF, Matz MV. 2010. Retracing the evolution of red fluorescence in GFP-like proteins from Faviina corals. *Mol Biol Evol*. 27: 225–233.

Fitch WM. 1971. Toward defining the course of evolution: minimum change for a specific tree topology. *Syst Zool*. 20:406–416.

Frentiu FD, Bernard GD, Cuevas CI, Sison-Mangus MP, Prudic KL, Briscoe AD. 2007. Adaptive evolution of color vision as seen through the eyes of butterflies. *Proc Natl Acad Sci U S A*. 104 (Suppl 1):8634–8640.

Frentiu FD, Bernard GD, Sison-Mangus MP, Brower AVZ, Briscoe AD. 2007. Gene duplication is an evolutionary mechanism for expanding spectral diversity in the long-wavelength photopigments of butterflies. *Mol Biol Evol*. 24:2016–2028.

Frentiu FD, Briscoe AD. 2008. A butterfly eye's view of birds. *Bioessays* 30:1151–1162.

Garrigan D, Lewontin RC, Wakeley J. 2010. Measuring the sensitivity of single-locus "neutrality tests" using a direct perturbation approach. *Mol Biol Evol*. 27:7389.

Guindon S, Gascuel O. 2003. A simple, fast, and accurate algorithm to estimate large phylogenies by maximum likelihood. *Syst Biol*. 52:696–704.

Hoekstra HE, Hirshmann RJ, Bundey RA, Insel PA, Crossland JP. 2006. A single amino acid mutation contributes to adaptive beach mouse color pattern. *Science* 313:101–104.

Hsu R, Briscoe AD, Chang BSW, Pierce NE. 2001. Molecular evolution of a long wavelength opsin in mimetic *Heliconius* butterflies (Lepidoptera: nymphalidae). *Biol J Linn Soc*. 72:435–449.

Kitamoto J, Sakamoto K, Ozaki K, Mishina Y, Arikawa K. 1998. Two visual pigments in a singe photoreceptor cell: identification and histological localization of three mRNAs encoding visual pigment opsins in the retina of the butterfly *Papilio xuthus*. *J Exp Biol*. 201:1255–1261.

Koshitaka H, Kinoshita M, Vorobyev M, Arikawa K. 2008. Tetrachromacy in a butterfly that has eight varieties of spectral receptors. *Proc Biol Sci*. 275:947–954.

Kumar S, Nei N, Dudley J, Tamura K. 2008. MEGA: a biologist-centric software for evolutionary analysis of DNA and protein sequences. *Brief Bioinform*. 9:299–306.

Maddison WP, Maddison DR. 2009. Mesquite: a modular system for evolutionary analysis. Version 2.72. Available from: http://mesquiteproject.org.

Mallet J, Beltran M, Neukirchen W, Linares M. 2007. Natural hybridization in heliconiine butterflies: the species boundary as a continuum. *BMC Evol Biol*. 7:28.

Messier W, Stewart CB. 1997. Episodic adaptive evolution of primate lysozymes. *Nature* 385:151–154.

Nathans J. 1990. Determinants of visual pigment absorbance: role of charged amino acids in the putative transmembrane segments. *Biochemistry* 29:937–942.

Nozawa M, Suzuki Y, Nei M. 2009. Reliabilities of identifying positive selection by the branch-site and the site-prediction methods. *Proc Natl Acad Sci U S A*. 106:6700–6705.

Nozawa M, Suzuki Y, Nei M. 2010. Is positive selection responsible for the evolution of a duplicate UV-sensitive opsin gene in *Heliconius* butterflies? *Proc Natl Acad Sci U S A*. 107:E96.

Palacios AG, Goldsmith TH, Bernard GD. 1996. Sensitivity of cones from a cyprinid fish (*Danio aequipinnatus*) to ultraviolet and visible light. *Vis Neurosci*. 13:411–421.

Palczewski K, Kumasaka T, Hori T, et al. (12 co-authors). 2000. Crystal structure of rhodopsin: a G protein-coupled receptor. *Science* 289:739–745.

Peitsch D, Feitz A, Hertel H, de Souza J, Ventura D, Menzel R. 1992. The spectral input systems of hymenopteran insects and their receptor-based colour vision. *J Comp Physiol*. 170:23–40.

Perry GH, Dominy NJ, Claw KG, et al. (13 co-authors). 2007. Diet and the evolution of human *amylase* gene copy number variation. *Nat Genet*. 39:1256–1260.

Pohl N, Sison-Mangus MP, Yee EN, Liswi SW, Briscoe AD. 2009. Impact of duplicate gene copies on phylogenetic analysis and divergence time estimates in butterflies. *BMC Evol Biol*. 9:99.

Posada D, Crandall KA. 1998. Modeltest: testing the model of DNA substitution. *Bioinformatics* 14:817–818.

Salcedo E, Farrell DM, Zheng L, Phistry M, Bagg EE, Britt SG. 2009. The green-absorbing *Drosophila* Rh6 visual pigment contains a blue-shifting amino acid substitution that is conserved in vertebrates. *J Biol Chem*. 284:5717–5722.

Salcedo E, Zheng L, Phistry M, Bagg EE, Britt SG. 2003. Molecular basis for ultraviolet vision in invertebrates. *J Neurosci*. 23:10873–10878.

Sauman I, Briscoe AD, Zhu H, Shi DD, Froy O, Stalleicken J, Yuan Q, Casselman A, Reppert SM. 2005. Connecting the navigational clock to sun compass input in the monarch butterfly brain. *Neuron* 46:457–467.

Sella G, Petrov DA, Przeworski M, Andolfatto P. 2009. Pervasive natural selection in the *Drosophila* genome? *PLoS Genet*. 5:e1000495.

Sison-Mangus MP, Bernard GD, Lampel J, Briscoe AD. 2006. Beauty in the eye of the beholder: the two blue opsins of lycaenid butterflies and the opsin gene-driven evolution of sexually dimorphic eyes. *J Exp Biol*. 209:3079–3090.

Sison-Mangus MP, Briscoe AD, Zaccardi G, Knüttel H, Kelber A. 2008. The lycaenid butterfly *Polyommatus icarus* uses a duplicated blue opsin to see green. *J Exp Biol*. 211:361–369.

Stalleicken J, Labhart T, Henrik M. 2006. Physiological characterization of the compound eye in monarch butterflies with focus on the dorsal rim area. *J Comp Physiol*. 192:321–331.

Stavenga DG, Numan JAJ, Tinbergen J, Kuiper JW. 1977. Insect pupil mechanisms. 2. Pigment migration in retinula cells of butterflies. *J Comp Physiol*. 113:73–93.

Storz JF, Runck AM, Sabatino SJ, Kelly JK, Ferrand N, Moriyama H, Weber RE, Fago A. 2009. Evolutionary and functional insights into the mechanism underlying high-altitude adaptation of deer mouse hemoglobin. *Proc Natl Acad Sci U S A*. 106:14450–14455.

Tamura K, Dudley J, Nei M, Kumar S. 2007. MEGA4: molecular evolutionary genetics analysis (MEGA) software version 4.0. *Mol Biol Evol*. 24:1596–1599.

Wakakuwa M, Stavenga DG, Arikawa K. 2007. Spectral organization of ommatidia in flower-visiting insects. *Photochem Photobiol*. 83:27–34.

Wheat CW, Haag CR, Marden JH, Hanksi I, Frilander MJ. 2010. Nucleotide polymorphism at a gene (*Pgi*) under balancing selection in a butterfly metapopulation. *Mol Biol Evol*. 27:267–281.

Wilkie SE, Robinson PR, Cronin TW, Poopalasundaram S, Bowmaker JK, Hunt DM. 2000. Spectral tuning of avian violet- and ultraviolet-sensitive visual pigments. *Biochemistry* 39:7895–7901.

Yang Z. 1998. Likelihood ratio tests for detecting positive selection and applications to primate lysozyme evolution. *Mol Biol Evol*. 15:568–573.

Yang Z-H. 2006. Computational molecular evolution. Oxford: Oxford University Press.

Yang Z-H, Wong WSW, Nielsen R. 2005. Bayes empirical Bayes inference of amino acid sites under positive selection. *Mol Biol Evol*. 22:1107–1118.

Yokoyama S, Radlwimmer FB. 1998. The 'five-sites' rule and the evolution of red and green color vision in mammals. *Mol Biol Evol*. 15:560–567.

Yokoyama S, Starmer WT, Takahashi Y, Tada T. 2006. Tertiary structure and spectral tuning of UV and violet pigments in vertebrates. *Gene* 365:95–103.

Yokoyama S, Tada T, Zhang H, Britt L. 2008. Elucidation of phenotypic adaptations: molecular analyses of dim-light vision proteins in vertebrates. *Proc Natl Acad Sci U S A*. 105:13480–13485.

Yokoyama S, Yang H, Starmer WT. 2008. Molecular basis of spectral tuning in the red- and green-sensitive (M/LWS) pigments in vertebrates. *Genetics* 179:2037–2043.

Yuan Q, Metterville D, Briscoe AD, Reppert SM. 2007. Insect cryptochromes: gene duplication and loss define diverse ways to construct insect circadian clocks. *Mol Biol Evol*. 24:948–955.

Zaccardi G, Kelber A, Sison-Mangus MP, Briscoe AD. 2006a. Color discrimination in the red range with only one long-wavelength sensitive opsin. *J Exp Biol*. 209:1944–1955.

Zaccardi G, Kelber A, Sison-Mangus MP, Briscoe AD. 2006b. Opsin expression in the eyes of *Heliconius erato*. *Perception* 35:142–143.

Zhang J, Kumar S, Nei M. 1997. Small-sample tests of episodic adaptive evolution: a case study of primate lysozymes. *Mol Biol Evol*. 14:11335–11338.

Zhang J, Nielsen R, Yang Z. 2005. Evaluation of an improved branch-site likelihood method for detecting positive selection at the molecular level. *Mol Biol Evol*. 22:2472–2479.

Zhang J, Rosenberg HF, Nei M. 1998. Positive Darwinian selection after gene duplication in primate ribonuclease genes. *Proc Natl Acad Sci U S A*. 95:3708–3713.